

Characterisation of a novel glycosylated glutathione transferase of *Onchocerca ochengi*, closest relative of the human river blindness parasite

Clair Rose¹; Giorgio Praulins¹; Stuart D. Armstrong²; Aitor Casas-Sanchez¹; Jem Davis¹; Gemma Molyneux¹; Cristina Yunta¹; Zenaida Stead¹; Mark Prescott³; Samirah Perally¹; Anne Rutter²; Benjamin L. Makepeace²; E. James La Course^{1*}; Alvaro Acosta-Serrano¹

¹Liverpool School of Tropical Medicine, UK; ²Institute of Infection & Global Health, University of Liverpool, UK; ³Institute of Integrative Biology, University of Liverpool, UK.

* Corresponding author

Key words: Immune modulation, glycans, GSTs, detoxification, *Onchocerca*, glycosylation, prostaglandin synthase

Affiliations

Clair.Rose@lstmed.ac.uk 0151 705 3727

Giorgio.Praulins@lstmed.ac.uk 0151 705 3397

sarmstro@liverpool.ac.uk

sanchez@lstmed.ac.uk

Jem.Davis@crl.com

gemma.molyneux@liverpool.ac.uk

cyuntayanes@hotmail.com

steadzena@gmail.com

mp1608@liverpool.ac.uk 0151 795 4485

samirahperally@gmail.com

anne.rutter@liverpool.ac.uk

blm1@liverpool.ac.uk 0151 794 1586

James.LaCourse@lstmed.ac.uk 0151 705 3153

Alvaro.Acosta-Serrano@lstmed.ac.uk 0151 705 3304

This is an Accepted Manuscript for Parasitology. This version may be subject to change during the production process. DOI: 10.1017/S0031182019000763

Abstract

Filarial nematodes possess glutathione transferases (GSTs), ubiquitous enzymes with potential to detoxify xenobiotic and endogenous substrates, and modulate the host immune system, which may aid worm infection establishment, maintenance and survival in the host. Here we have identified and characterised a sigma class glycosylated GST (OoGST1), from the cattle-infective filarial nematode *Onchocerca ochengi*, which is homologous (99% amino acid identity) with an immunodominant GST and potential vaccine candidate from the human parasite, *O. volvulus*, (OvGST1b). *O. ochengi* native GSTs were purified using a two-step affinity chromatography approach, resolved by 2D and 1D SDS-PAGE and subjected to enzymic deglycosylation revealing the existence of at least four glycoforms. A combination of lectin-blotting and mass spectrometry (MS) analyses of the released *N*-glycans indicated that OoGST1 contained mainly oligomannose Man₅GlcNAc₂ structure, but also hybrid- and larger oligomannose-type glycans in a lower proportion. Furthermore, purified OoGST1 showed prostaglandin synthase activity as confirmed by Liquid Chromatography (LC)/MS following a coupled-enzyme assay. This is only the second reported and characterised glycosylated GST and our study highlights its potential role in host-parasite interactions and use in the study of human onchocerciasis.

Accepted Manuscript

Introduction

The cattle filarial nematode *Onchocerca ochengi* is a well-established model natural system for the study of human onchocerciasis, the causative agent of which is *O. volvulus* (Trees 1992, Makepeace and Tanya 2016). Onchocerciasis is a devastating, vector borne, neglected tropical disease, affecting over 15 million people, 99% of whom live in Africa. Symptoms range from severe itching and disfiguring skin conditions (for the majority of sufferers), to being the second-leading infectious cause of blindness in Africa at over 1 million afflicted with vision loss (WHO 2018). In efforts to discover new ways to control onchocerciasis, much research has been focused on the molecules which may allow *Onchocerca* spp. to establish and maintain infection. One such protein family is the glutathione transferases (GSTs) which may aid worm survival through detoxification of drugs and evasion of host-derived immunochemical attack, and with the potential to play roles in immunomodulation (Chasseaud 1979, Jakoby and Habig 1980, Brophy and Barrett 1990, Sheehan, Meade et al. 2001, Sommer, Rickert et al. 2003, Hayes, Flanagan et al. 2005). Initial explorations of the *Onchocerca* spp genomes reveal a glutathione transferase (OoGST1 – Accession, nOo.2.0.1.t09064) from *O. ochengi* (Armstrong, Xia et al. 2016), displaying 99% amino acid identity with an immunodominant GST (OvGST1b - Accession AAG44696.1) (Liebau, Wildenburg et al. 1994, Alhassan, Makepeace et al. 2014) and potential vaccine candidate from the closely related human parasite *O. volvulus* (Graham, Wu et al. 1999). OvGST1b and its paralogous gene product OvGST1a (AAG44695.1) are exceptional within the GST superfamily in being glycosylated, having a cleavable signal peptide and N-terminal extension not found in other GSTs, though the roles of these novel features and glycosylation are yet to be fully elucidated (Sommer, Rickert et al. 2003, Perbandt, Hoppner et al. 2008). The potential of these inherent glycans to function in, as yet undefined, roles at the host-parasite interface are of particular interest given OvGST1b is shown to have prostaglandin synthase activity and so may possess the ability to modulate the host immune response to filarial infection (Sommer, Rickert et al. 2003, Perbandt, Hoppner et al. 2008). Furthermore, a deeper knowledge of protein glycosylation has important implications for future vaccine development and an understanding of host-parasite interactions. Whilst most screening of parasite products for immunoreactive vaccine candidate antigens is predominantly protein focused (Diemert, Bottazzi et al. 2018), antibody responses to glycosylated proteins demonstrates the high immunogenicity of glycan extensions, highlighting clear rationale for a greater attention (Jaurigue and Seeberger 2017).

Extending such focus on OvGST1b in the human-infecting *O. volvulus* filarial worm is however significantly limited through obvious logistical aspects in access to worm samples and necessary ethical constraints. Many onchocerciasis studies thus employ the closely related *O. ochengi* species in cattle as a valuable and accessible model for research into the genes and proteins which may play roles in this disease (Trees, Graham et al. 2000). *O. ochengi* GST homologue OoGST1 however, has

yet to be isolated and studied to validate its status in terms of comparable structure, glycosylation state and enzymic activity with that of OvGST1b.

Therefore, investigations to resolve *O. ochengi* GSTs, characterise enzymic activity and unravel the structure of *N*-glycan modifications of the homologous OoGST1 protein, are presented here to allow comparative exploration of potential roles in host-parasite interactions. Our findings reveal subtle differences in glycosylation state between OvGST1s and OoGST1.

Materials and Methods

Parasite material

O. ochengi adult female gravid worms were collected from nodules in hides of infected Gudali cattle from the Ngaounédré abattoir in the Adamawa region of Cameroon. Worm masses were dissected from collagenous tissue within nodules and male worms were removed. The females were washed in PBS and separated into 2 mL cryovial tubes before freezing and storage at -80°C. Isolated female worms were transported to the UK on dry ice.

Glutathione transferase purification

Cytosolic extracts from *O. ochengi* were obtained by homogenisation of frozen worms in an ice-cooled glass grinder in buffer containing 20 mM potassium phosphate, pH 7.0, 0.2% Triton X-100, 5 mM DTT and a cocktail of protease inhibitors (Roche, Mini-Complete, EDTA-free). Following homogenisation, samples were centrifuged at 100,000 × *g* for 1 h at 4 °C and the supernatant, termed the cytosolic fraction, was retained for purification of GSTs.

GSTs were partially purified and further resolved to isolate glycosylated forms from the cytosolic fraction in two steps; 'Step 1' employed *S*-hexylglutathione-affinity (*S*-hexylGSH-affinity) chromatography according to the adapted method of (Simons and Vander Jagt 1977). In brief, the *O. ochengi* cytosolic fraction was passed at 0.5 mL/min through Econo-columns (1.0 x 5 cm, 4 mL Bio-Rad, U.K.), containing 1 mL of *S*-hexylGSH-agarose (Sigma Aldrich), re-hydrated according to manufacturer's instructions and equilibrated with 20 mL of 20 mM potassium-phosphate buffer pH 7.0, 50 mM NaCl (equilibration buffer). Non-*S*-hexylGSH-affinity proteins were washed from the column with 20 mL equilibration buffer at 0.5 mL/min. Affinity-bound proteins were eluted in 3 mL 50 mM Tris-HCl pH 8.0 buffer, containing 2 mM *S*-hexylGSH, and concentrated via centrifugal filtration in 10 kDa molecular weight cut off filters (Amicon Ultra-4, Millipore). GST samples were reduced to a final volume of 100 µL through three successive cycles of ten-fold dilutions/centrifugal reductions in 50 mM Tris-HCl pH 8.0 to remove proteins, free glutathione and low molecular mass substances of a native weight below 10 kDa.

The partially purified pool of GSTs obtained in 'Step 1' was incubated with a range of different lectins to determine optimum lectin selection for 'Step 2' isolation of glycosylated GST from the GST pool. Glycosylated GSTs were isolated from the partially purified pool of GSTs obtained in 'Step 1' via lectin-affinity chromatography using concanavalin A-agarose (Sigma Aldrich) according to the manufacturer's instructions.

Glutathione transferase enzyme activity

Establishment of GST presence within *O. ochengi* cytosolic extracts and S-hexylglutathione-binding protein samples was assayed via enzyme activity at 25 °C over 3 min at 340 nm using 1 mM 1-chloro-2, 4-dinitrobenzene (CDNB) as standard second substrate in 100 mM potassium phosphate pH 6.5, containing 1 mM reduced glutathione in accordance with the adapted method of Habig et al, (Habig, Pabst et al. 1974). Assays were undertaken in triplicate in a Cary Varian spectrophotometer with specific activity expressed as nmol GSH/CDNB conjugated min⁻¹ mg⁻¹ protein (± standard deviation), and calculated as described by (Barrett 1997) (see Equation 1 below):

Equation 1.

$$\frac{\Delta OD}{\epsilon \times t} \times V \times L \times \frac{1}{Pr} \times \frac{1}{S} \times 10^n = \text{Specific Activity (nmol.min}^{-1} \cdot \text{mg protein}^{-1})$$

(Key to Equation 1. ΔOD = change in optical density over time (t) in minutes.; ϵ = extinction coefficient.; V = total volume of assay mixture in the cuvette (mL).; L = path length of the cuvette in cm.; Pr = protein concentration of enzyme extract (mg/mL).; S = volume of enzyme extract added to cuvette (ml). ; The value of n is dependent on the extinction coefficient (ϵ): If ϵ is in cm².M⁻¹, then n = 9, If ϵ is in M⁻¹.cm⁻¹, then n = 6, If ϵ is in mM⁻¹.cm⁻¹, then n = 3)

Protein concentrations were estimated via the adapted method of Bradford (Bradford 1976) using the Sigma (UK) Bradford Reagent protocol according to the manufacturer's instructions.

Electrophoresis

Two-dimensional gel electrophoresis (2DE)

20 µg of native purified GSTs (S-hexylglutathione-binding proteins) was resuspended into immobilised pH gradient (IPG) rehydration buffer (6 M urea, 1.5 M thiourea, 3% w/v CHAPS, 66 mM DTT, 0.5% v/v ampholytes pH 3–10 (Pharmalytes, Amersham BioSciences, UK)) to a final volume of 300 µl. In-gel passive rehydration and isoelectric focusing of IPG gel strips with protein samples was at 20 °C with mineral oil overlay according to IPG strip manufacturer's instructions (Bio-Rad, UK). Isoelectric focused strips were equilibrated, in two stages: a 'reducing stage' for 15 min in 'equilibration buffer' (50 mM

Tris–HCl pH 8.8, 6 M urea, 30% glycerol, 2% SDS) containing 1% (w/v) DTT, followed by a 15 min ‘alkylating stage’ in ‘equilibration buffer’ containing 2.5% (w/v) iodoacetamide replacing 1% DTT (LaCourse, Hernandez-Viadel et al. 2009). Gels were then fixed overnight in 40% methanol/10% acetic acid, stained in colloidal Coomassie Blue G-250 overnight and then de-stained in 1% acetic acid.

Sodium dodecyl sulphate polyacrylamide gel electrophoresis (SDS-PAGE)

Protein samples were resolved by SDS-PAGE according to methods adapted from Laemmli (Laemmli 1970) on 12.5% polyacrylamide gels as previously described (LaCourse, Hernandez-Viadel et al. 2009). Gels were Coomassie or Periodic-acid Schiff (PAS) stained (Sigma) and scanned upon a GS-800 densitometer (Bio-Rad).

Quadrupole Time of Flight (QToF) Tandem Mass Spectrometry (MS/MS) analysis of OoGST peptides

Tryptic peptides were generated as previously described (LaCourse, Hernandez-Viadel et al. 2009). Peptide mixtures from trypsin digested gel spots were separated using a LC Packings Ultimate nano-HPLC System. Sample injection was *via* an LC Packings Famos auto-sampler and the loading solvent was 0.1% formic acid. The pre-column used was a LC Packings C18 PepMap 100, 5 mm, 100A and the nano HPLC column was a LC Packings PepMap C18, 3 mm, 100A. The solvent system was: solvent A 2% ACN with 0.1% formic acid, and solvent B, 80% ACN with 0.1% formic acid. The LC flow rate was 0.2 ml/min. The gradient employed was 5% solvent A to 100% solvent B in 1 hour. The HPLC eluent was sprayed into the nano-ES source of a Waters Q-TOF μ MS *via* a New Objective Pico-Tip emitter. The MS was operated in the positive ion ES mode and multiple charged ions were detected using a data-directed MS-MS experiment. Collision induced dissociation (CID) MS-MS mass spectra were recorded over the mass range m/z 80-1400 Da with scan time 1 s. The raw MS-MS spectral data files were processed using Waters ProteinLynx software (Waters, UK) to produce Sequest dta file lists which were then merged into a Mascot generic format (mgf) file.

Protein identification

Raw MS/MS files were converted into mgf files using MSconvert component of the ProteoWizard (V 3.0) tool (Chambers, Maclean et al. 2012). All tandem MS data generated were searched against partially revised *Onchocerca ochengi* gene models based on data downloaded from WormBase ParaSite (Armstrong, Xia et al. 2016) and a *Bos taurus* reference proteome (UniProt UP000009136, March 2019) (37957 sequences, 17775113 residues in total) using the search engine MASCOT (version 2.3.02, Matrix science) Search parameters were a precursor mass tolerance of ± 1.2 Da and fragment mass tolerance of ± 0.6 Da. One missed cleavage was permitted, carbamidomethylation was

set as a fixed modification and oxidation (M) and deamidation (N, Q) were included as variable modifications. Individual ion scores ≥ 39 were considered to indicate identity or extensive homology ($p < 0.05$), using MudPIT scoring. Only proteins with > 2 peptides were used for analysis. Data were deposited to the PRIDE repository (Vizcaino, Csordas et al. 2016) with the data set identifier PXD013440.

Glycan analysis of *O. ochengi* sigma class GST

Enzymic de-glycosylation of GSTs

GST samples were de-glycosylated with either peptide N^4 -(N-acetyl- β -glucosaminy) asparagine amidase F (PNGase F) or endoglycosidase H (Endo H) (both from NEB) treatment under reducing conditions according to the manufacturer's instructions. Briefly, 0.4 $\mu\text{g}/\mu\text{l}$ OoGST and 1 $\mu\text{g}/\mu\text{l}$ of glycosylated egg albumin (as positive control) were denatured at 100 °C for 10 min in Glycoprotein Denaturing Buffer. NP-40 was then added for PNGase F treatment only and samples digested with 25 units/ μl per enzyme overnight in a 37 °C water bath. Mock-treated samples were processed the same (but without the addition of any enzyme) and the reactions were stopped by heating. All protein samples were fractionated by SDS-PAGE and either Coomassie blue or PAS stained or used for lectin blotting as indicated below.

Lectin-blotting

Lectin blotting was performed according to methods adapted from (Luk, Johnson et al. 2008). Approximately 1 μg of PNGase F-treated or untreated sigma class OoGST (see above) was fractionated on a 12.5% SDS-PAGE gel as described previously and transferred onto polyvinylidene fluoride (PVDF) membranes at 90 V for 30 minutes on ice. The membranes were then incubated overnight at 4 °C in blocking buffer (PBS, 0.1% (v/v) Tween 20, 1% (w/v) BSA). Following several washes in washing buffer (PBS/0.1% (w/v) Tween 20), each membrane was incubated with 1 $\mu\text{g}/\text{ml}$ biotinylated concanavalin A (ConA) (Vector Labs) for 1 hour at room temperature (20-23°C). Following further washes, membranes were then incubated in streptavidin-horse radish peroxidase (HRP) (ThermoFisher) at a 1:100,000 dilution for 1 hour at room temperature (20 - 23°C). Membranes were washed and then incubated with SuperSignal West Dura (Pierce, UK) peroxidase buffer and luminol:enhancer solution at a 1:1 ratio, and developed by chemiluminescence, which continued for up to 5 hours.

Glycan structural analysis

N-glycans from OoGST were released by PNGase F and purified by gel filtration chromatography as indicated in (Kozak, Tortosa et al. 2015). Hydrophilic Interaction Liquid Chromatography–Ultra high-performance liquid chromatography (HILIC-UHPLC) analysis was performed using a Dionex Ultimate 3000 UHPLC instrument. The conditions included using a BEH-Glycan 1.7 32 µm and 2.1 x 150 mm column at 40°C, with a fluorescence detector (Lamdaex = 310 nm and lamdaem = 370 nm). These conditions were controlled by Bruker HyStar 3.2 buffer A (50 mM ammonium formate pH 4.4) and Buffer B (acetonitrile). Sample volume for injection was 25 µl, at a ratio of 24% and 76% acetonitrile. Glucose unit (GU) values of peaks were assigned by chameleon 7.2 data software with a cubic spline fit. The system standard and the GU calibration standard was a glucose homopolymer labelled with procainamide. The mass spectra were collected in a Bruker AmaZon Speed ETD electrospray mass spectrometer, performed immediately after the UHPLC fluorescence detector without splitting. Samples were scanned in maximum resolution mode, positive ion settings, MS scan + three MS/MS scans. The MS/MS scans were done on three ions in each scan sweep with a mixing time of 40 ms at a nebuliser pressure of 14.5 psi, a nitrogen flow of 10 litres/min and using 4500 V capillary voltage.

Prostaglandin-synthase assay

Prostaglandin synthase activity was assessed via the composite method of LaCourse et al (LaCourse, Perally et al. 2012) based upon aspects adapted from the original methods of Sommer et al. (Sommer, Rickert et al. 2003) and Meyer et al. (Meyer and Thomas 1995, Meyer, Muimo et al. 1996), with extraction modifications based upon Schmidt (Schmidt, Coste et al. 2005).

Sequence analysis of *O. ochengi* glycosylated glutathione transferase OoGST1

O. ochengi glycosylated sigma-class GST (OoGST1) amino acid sequence (accession number nOo.2.0.1.t09064) was obtained from the University of Edinburgh's *O. ochengi* genome assembly v. nOo.2.0.1 hosted by WormBase ParaSite (Howe, Bolt et al. 2017, Consortium 2019). *O. ochengi* GST Oo_GST_t09064 was aligned to highlight key residues involved in prostaglandin H₂ binding using ClustalX Version 2.1 (Thompson, Gibson et al. 1997, Larkin, Blackshields et al. 2007) with homologues Ov_GST_Ia (AAG44695.1) and Ov_GST_Ib (AAG44696.1) from *O. volvulus* along with the two mammalian haematopoietic prostaglandin D synthases (PGDS), highlighted in (Perbandt, Hoppner et al. 2008).

Structural analysis of OoGST1

Initial protein tertiary models of *O. ochengi* sigma class GST were produced *in silico* using SwissModel (Arnold, Bordoli et al. 2006) and Phyre2 (Kelley, Mezulis et al. 2015) with prostaglandin D synthase of

O. volvulus (Protein Data Bank (PDB) 2HNL) used as a template structure. Homology prediction was also carried out by RaptorX (Kallberg, Wang et al. 2012) to predict disordered amino acid regions and I-Tasser (Yang, Yan et al. 2015) for increased confidence before refinement of the predicted model via ModRefiner (Xu and Zhang 2011). Final structures were modified in PyMol (DeLano 2002).

Results

Sequence analyses and homology prediction

OoGST1 shares 99% and 96% identity to *O. volvulus* GST1b and 1a respectively (Fig. 1a). All three nematode GSTs are sigma class, have a 25-amino acid signal peptide that is cleaved prior to maturation and possess a 25-amino acid N-terminal extension not found in any other GST to date. Sequence similarity to other sigma class GSTs commences after this extension and, like OvGST1b, OoGST1 shows 32% and 35% identity to the human and rat haematopoietic prostaglandin D synthase (PGDS), respectively (accession numbers gi:30749302 and gi:6435744). Similarly, the proposed prostaglandin H₂ binding pocket differs significantly between the mammalian and *Onchocerca* GSTs and may suggest a potentially different binding mode for OoGST1 and OvGST1b than for the rat and Homo PGDS (Perbandt, Hoppner et al. 2008).

There are also 6 potential *N*-glycosylation sites in OoGST1: one in the signal peptide (Asn⁵), one in the N-terminal extension (Asn⁷), two in the N-terminus (Asn⁵⁰, Asn⁷⁹), and two in the C-terminus (Asn¹³⁴, Asn¹⁴⁴) of the mature protein. Homology modelling of OoGST1 predicts, in accordance with other sigma class GSTs, that this enzyme forms a dimeric protein (Fig. 1b). However, each homodimer possesses a 'lock and key' mechanism, typically observed only in other GST classes (alpha, mu, pi) and vertebrate PGDS, but not normally observed in other nematodes aside from OvGST1b previously (Inoue, Irikura et al. 2003, Line, Isupov et al. 2019). Additionally, although topologically similar to pi class GSTs, the structural differences in the substrate binding pocket of OoGST1 causes significant conformity changes resulting in a wider, shallower cleft.

The primary structure of the unusual 25 amino acid N-terminus extension is composed of a higher percentage (68%) of disorder-promoting amino acids; Ala, Arg, Gly, Gln, Ser, Glu, Lys and Pro, a low content of hydrophobic residues (12%), and no aromatic residues. This combination of amino acids suggests this part of the protein is unable to form the well-organised hydrophobic core that makes up a structured domain and thus is predicted to be an intrinsically disordered region (IDR) (Uversky 2013). Indeed, x-ray crystallography of the OvGST1a on which this model was based revealed that this region lacked electron density and was therefore not modelled (Perbandt, Hoppner et al. 2008).

Purification and enzymic characterisation of OoGST

O. ochengi GST proteins from gravid, adult female worms were purified by affinity chromatography as described in Materials and Methods, and the enzymic activity carried out as shown by (Habig, Pabst et al. 1974, Simons and Vander Jagt 1977). Using CDNB as a model substrate, we found significant differences in cytosolic GST activity between whole worm extract, affinity-purified and column flow through (non-affinity) of 0.008, 1.310 and 0.001 $\mu\text{mol}\cdot\text{min}^{-1}\cdot\text{mg}^{-1}$, respectively (supplementary table 1). A 171-fold purification of GSTs was obtained, with a yield of almost 40% of the total GST activity content collected.

Analysis of *O. ochengi* GSTs by 2DE

Considering that *O. ochengi* is predicted to have several GST classes (Armstrong, Xia et al. 2016), we carried out 2DE (Fig. 2) in order to resolve the GST classes for mass spectrometry protein identification (table 1 and supplementary file 1). Whilst pi class GSTs are shown around the 25 kDa mark, but with different isoelectric points, sigma class GSTs migrated at a higher apparent molecular mass (~35 kDa), but with spots less well-resolved than the pi class isoforms. This indicates that sigma class GST proteins were post-translationally modified, most likely glycosylated (see below).

Proteins were then excised from gels and identified by mass spectrometry in conjunction with MS-MS ions searches of a partially revised, publicly available *O. ochengi* protein sequence databases (Armstrong, Xia et al. 2016). Proteins identified were almost exclusively of the pi and sigma classes of GSTs (table 1 and supplementary file 1). As expected, we also identified bovine proteins, including a pi-class GST in several spots (supplementary file 1).

***O. ochengi* GSTs are *N*-glycosylated and mainly modified by oligomannose *N*-glycans**

To verify that sigma class GSTs were glycosylated, as predicted by the presence of several *N*-glycosylation sequons (5-6) and also suggested by their migration on 2DE gels, S-hexylGSH-affinity-purified GSTs were incubated with either PNGase F or Endo-H. After digestion, only sigma class GSTs appeared susceptible to either enzyme, as indicated by their faster migration on a Coomassie-stained gel (Fig 3a and 3b). Furthermore, the lack of PAS reactivity after PNGase F treatment suggests that these proteins are specifically *N*-glycosylated (Fig. 3a, lanes 3 and 4). Whilst PNGase F caused a shift in migration of ~10 kDa, samples treated with Endo-H yield an extra band of ~28 kDa suggesting the possible presence of fucosylated, hybrid- or complex-type glycans on these proteins (Fig. 3b, lane 2). The identity of all GST proteins, before or after deglycosylation, was confirmed by mass spectrometry (not shown).

***O. ochengi* GST are mainly modified by mannosylated *N*-glycans**

To further determine the types of *N*-glycans present on *O. ochengi* GST, lectin-blotting was carried out using ConA for the recognition of terminal α -mannose residues (Fig. 4). As expected, in untreated sample, ConA recognised all the sigma class GSTs, which migrated ~35-40 kDa, although recognition of a band with an apparent molecular mass of ~25 kDa, suggests some degradation may have occurred (Fig. 4a). Following digestion with PNGaseF, most of the ConA binding was lost.

We took advantage of ConA recognition of the *O. ochengi* sigma class GSTs for protein purification and glycan structural analyses. After total *O. ochengi* GSTs were enriched by affinity chromatography using an S-hexylGSH column, only the glycosylated, sigma class GSTs bound and were eluted off from the ConA column (Fig. 5). These samples were subsequently digested with PNGase F and the released glycans tagged with procanamide and analysed by HILIC-liquid chromatography followed by ESI-MS and ESI-MS/MS. As shown in Fig. 6, the Man₅GlcNAc₂-Proc structure represents the main glycan species (~45%) from sigma class OoGST. This was confirmed by positive-ion EIS-MS analysis, which showed the presence of abundant [M+H⁺] and [M+H⁺]²⁺ pseudomolecular ions at *m/z* 1454.8 and 727.9, respectively, corresponding to a glycan of composition Hex₅HexNAc₂-Proc (Fig. S1 and table 2). In addition, short paucimannose structures (Man₄GlcNAc₂-Proc and Man₃GlcNAc₂-Proc), oligomannoses (Man₆₋₉GlcNAc₂-Proc) and a few hybrid-type species (e.g. Fuc₁Man₃GlcNAc₂-Proc and Man₃GlcNAc₃₋₄-Proc) were found (table 2). The identity of all glycan species, including that of the Man₅GlcNAc₂-Proc oligosaccharide, was further corroborated by MS/MS analyses, which produced the characteristic fragment ions (Fig. 7a and b).

OoGST1 displays prostaglandin synthase activity

Sigma class GSTs have previously been reported to synthesise prostaglandin D₂ (PGD₂), PGE₂ and PGF₂; eicosanoids that function in diverse physiological systems and pathological processes (Meyer and Thomas 1995, Sommer, Rickert et al. 2003). Using the ConA-affinity-purified *O. ochengi* GST fraction shown to contain only OoGST1 (Fig. 5, lane 3) we employed a coupled assay with cyclooxygenase (COX-1) and arachidonic acid which showed OoGST1 also has the ability to synthesise prostaglandins. Nano-LC/MS detected the presence of both PGD₂ and PGE₂ in the assay mixture with the PGD₂ form being the more significantly abundant of the two eicosanoids (Fig. 8). OoGST1 appears to reflect a similar proportionality and specificity to catalyse predominantly, or only PGD₂ from PGH₂, in a concentration-dependent manner as described for OvGST1a (Sommer, Rickert et al. 2003). The presence of PGE₂, a relatively limited product observed, may, as proposed by Sommer et al, (2003) represent by-product of rapid degradation of the highly unstable PGH₂.

Discussion

The sigma class GST of *O. ochengi* is of particular interest in terms of the potential involvement in host immune modulation as well as possible roles in detoxification of other endogenous host- and parasite-derived toxins. Given the presence of a signal peptide and its detection at the host-parasite interface in bovine nodule fluid (Armstrong, Xia et al. 2016), suggesting probable roles in the long-term survival of the parasite, further investigation of this GST in *O. ochengi* is warranted. Furthermore, the ability of GSTs to detoxify endogenous and exogenous compounds, although well researched in other organisms, has not been fully explored in *O. ochengi*; that is, how any Phase II function may facilitate parasite establishment or survival.

We also show the predicted homology model between OvGST1a and OoGST1 is almost identical, with both homodimers forming a dimeric functional protein. The significance of the 25-amino acid disordered region that both GSTs possess is yet to be determined. Intrinsically disordered proteins (IDPs) and proteins containing IDRs lack stable tertiary and/or secondary structures under physiological conditions, but are nevertheless fully functional and actively participate in diverse functions mediated by proteins (Dunker, Silman et al. 2008, van der Lee, Buljan et al. 2014). These functions include cell signalling, cell regulation, molecular recognition and have also been shown to modulate immune responses (Wright and Dyson 2015). Recent evidence has shown that parasites such as *Schistosoma mansoni*, *Plasmodium falciparum* and *Toxoplasma gondii* overexpress several predicted disordered protein families, with transcripts more abundant in life stages that are exposed to the mammalian host immune system (Feng, Zhang et al. 2006, Lopes, Orcia et al. 2013, Ruy, Torrieri et al. 2014). Moreover, some of these families undergo disordered-to-ordered transitions in response to the external environmental conditions and have been shown to interact and bind with human immunomodulatory proteins (Lopes, Orcia et al. 2013).

Although not tested here, the disordered region of OoGST1 may facilitate the way in which the GST is inserted at the host-parasite interface in the cuticular basal layer and the outer layer of the hypodermis. Interestingly, OoGST1 is the only sigma-class *O. ochengi* GST that is expressed in all parasite life stages (Armstrong, Xia et al. 2016). Whilst several additional sigma-class GSTs were previously detected in a shotgun proteomic analysis of the whole *O. ochengi* lifecycle, their absence in the current LC-MS study suggests they are expressed at a much lower level than OoGST1.

Here we have demonstrated that OoGST1 is able to synthesise two prostaglandins; PGD2 and PGE2. In line with studies on the *O. volvulus* OvGST1a (Sommer, Rickert et al. 2003) PGD2 appears to predominate as the major isomerisation product of the reaction. Research highlights the potential for prostaglandins to be involved in a variety of host-parasite interactions and roles including reproduction, inflammatory responses and immunomodulation, yet much still remains to be understood; specifically, how these mechanisms and roles may relate to GSTs in helminth parasites and their interactions with mammalian hosts (Dauguschies and Joachim 2000, Szkudlinski 2000, Brattig, Schwohl et al. 2006, Kubata, Duszenko et al. 2007, Biserova, Kutyrev et al. 2011, Joachim and Ruttkowski 2011, Sankari,

Hoti et al. 2013, Kuttyrev, Biserova et al. 2017, Laan, Williams et al. 2017). Several reports highlight potential involvement of eicosanoids in filarial worm infections. For example, Sommer et al (2003) propose microfilariae of *O. volvulus* present in the skin of humans may employ PGD2 to avoid the cutaneous immune response in a similar way to that demonstrated by Angeli et al (2001) in the *Schistosoma mansoni*-mouse model of human infection. Lui & Weller (1992) demonstrate prostanoids secreted by *Brugia malayi* inhibited host platelet aggregation, whilst production of PGD2 in supernatant of *Dirofilaria immitis* indicted involvement in the relaxation of the aorta during canine heartworm disease. Further studies exploring the potential of *Onchocerca*-derived PGD2 to modulate the host immune system are currently underway in our laboratory.

Our lectin-binding and structural analyses demonstrated that OoGST1 is a glycosylated protein. The expression of glycosylated GSTs has previously only been observed in the closely related filarial nematode, *O. volvulus*. OvGST1a and OvGST1b share 96% and 99% identity, respectively, to *O. ochengi* OoGST1, although the latter has an additional potential *N*-glycosylation sequon in the N-terminus. A combination of HILIC chromatography and LC-EIS-MS/MS of procainamide-labelled glycans showed that OoGST1 is mainly modified by a Man₅GlcNAc₂ oligosaccharide and, in a lower proportion, a series of larger oligomannose structures (i.e. Man₆₋₉GlcNAc₂). This is similar to the glycan profile observed in glycopeptides from OvGST1 (Sommer, Nimitz et al. 2001). Interestingly, we found that OoGST1 also contains a fucosylated hybrid-type structure, with the fucose residue potentially linked as $\alpha(1-3)$ to innermost GlcNAc residue (based on PNGase F sensitivity). Previous studies have shown that *N*-glycans containing an $\alpha(1-3)$ fucose residue are common in helminth glycoproteins, which are highly immunogenic and elicit TH2 immune responses (Faveeuw, Mallevaey et al. 2003). It remains to be determined whether the presence of fucosylated glycans renders OoGST1 more immunogenic. Interestingly, OvGST1 *N*-glycans appear to render this protein more immunogenic to humans infected with *O. volvulus*, although no fucosylated glycans were detected by mass spectrometry (Sommer, Nimitz et al. 2001). Whilst the role of OoGST *N*-glycans remains to be determined, one potential function could be to increase its solubility in animal serum. Furthermore, the predominant presence of oligomannose structures could facilitate recognition by immune cells receptors with lectin domains, like the mannose receptor and DC-SIGN (Guo, Feinberg et al. 2004, Taylor, Martinez-Pomares et al. 2005).

Following this initial characterisation of OoGST1, the opportunity exists for a wider range of studies upon this enzyme within the *O. ochengi* cattle experimental model system to inform studies of onchocerciasis and subsequent application to the human parasite *O. volvulus*. Indeed, cloning, expression and crystallographic studies, explorations of immunological aspects, as well as biochemical characterisations with a range of natural and model substrates, are underway with this glycosylated sigma class GST of *O. ochengi*.

Acknowledgements

We thank Dr Richard Gardener and Dr Daniel Spencer (Ludger, Oxford) for performing the glycan analysis. We are grateful to the field team led by Dr Germanus Bah and Dr Vincent Tanya at the Institut de Recherche Agricole pour le Développement, Regional Centre of Wakwa, for co-ordinating the supply of worm material.

Financial Support

SDA and BLM were supported by the 7th Framework Programme of the European Commission (project identifier HEALTH-F3-2010-242131). ACS was supported by GlycoPar-EU FP7 Marie Curie Initial Training Network (GA. 608295) (Awarded to ACS and AAS; www.ec.europa.eu). GP, JD, ZS and AR were supported by LSTM MSc Degree research project funding.

Author Contributions

EJL, CR, BLM, AAS conceived and designed the experiments:

EJL, CR, GP, ACS, JD, GM, CYY, MP, SP, AR, ZS performed the experiments:

EJL, CR, GP, SDA, JD, GM, CYY, MP, SP, AR, BLM, AAS, ZS analysed the data:

EJL, BLM, AAS contributed reagents/materials/analysis tools:

EJL, CR, GP, SDA, GM, CYY, MP, BLM, AAS wrote the paper:

ORCID IDs: EJL, 0000-0001-9261-7136; CR, 0000-0001-7782-5359; GP, 0000-0003-2601-2598; BLM, 0000-0002-6100-6727; AAS, 0000-0002-2576-7959; ACS, 0000-0001-5237-1223.

Conflicts of Interest

None

Ethical Standards

Not applicable

References

- Alhassan, A., B. L. Makepeace, E. J. LaCourse, M. Y. Osei-Atweneboana and C. K. Carlow (2014). "A simple isothermal DNA amplification method to screen black flies for *Onchocerca volvulus* infection." *PLoS One* **9**(10): e108927.
- Angeli, V., C. Faveeuw, O. Roye, J. Fontaine, E. Teissier, A. Capron, I. Wolowczuk, M. Capron, and F. Trottein. 2001. Role of the parasite-derived prostaglandin D2 in the inhibition of epidermal Langerhans cell migration during schistosomiasis infection. *J. Exp. Med.* 193:1135–1147.
- Armstrong, S. D., D. Xia, G. S. Bah, R. Krishna, H. F. Ngangyung, E. J. LaCourse, H. J. McSorley, J. A. Kengne-Ouafu, P. W. Chounna-Ndongmo, S. Wanji, P. A. Enyong, D. W. Taylor, M. L. Blaxter, J. M. Wastling, V. N. Tanya and B. L. Makepeace (2016). "Stage-specific Proteomes from *Onchocerca ochengi*, Sister Species of the Human River Blindness Parasite, Uncover Adaptations to a Nodular Lifestyle." *Molecular & cellular proteomics : MCP* **15**(8): 2554-2575.
- Arnold, K., L. Bordoli, J. Kopp and T. Schwede (2006). "The SWISS-MODEL workspace: a web-based environment for protein structure homology modelling." *Bioinformatics* **22**(2): 195-201.
- Barrett, J. (1997). *Biochemical Pathways in Parasites. Analytical Parasitology*. M. T. Rogan. Berlin, Heidelberg, Springer Berlin Heidelberg: 1-31.
- Biserova, N. M., I. A. Kutyrev and V. V. Malakhov (2011). "The tapeworm *Diphyllobothrium dendriticum* (Cestoda) produces prostaglandin E2, a regulator of host immunity." *Dokl Biol Sci* **441**: 367-369.
- Bradford, M. M. (1976). "A rapid and sensitive method for the quantitation of microgram quantities of protein utilizing the principle of protein-dye binding." *Analytical Biochemistry* **72**(1): 248-254.
- Brattig, N. W., A. Schwohl, R. Rickert and D. W. Buttner (2006). "The filarial parasite *Onchocerca volvulus* generates the lipid mediator prostaglandin E(2)." *Microbes Infect* **8**(3): 873-879.
- Brophy, P. M. and J. Barrett (1990). "Glutathione transferase in helminths." *Parasitology* **100 Pt 2**: 345-349.
- Chambers, M. C., B. Maclean, R. Burke, D. Amodei, D. L. Ruderman, S. Neumann, L. Gatto, B. Fischer, B. Pratt, J. Egertson, K. Hoff, D. Kessner, N. Tasman, N. Shulman, B. Frewen, T. A. Baker, M. Y. Brusniak, C. Paulse, D. Creasy, L. Flashner, K. Kani, C. Moulding, S. L. Seymour, L. M. Nuwaysir, B. Lefebvre, F. Kuhlmann, J. Roark, P. Rainer, S. Detlev, T. Hemenway, A. Huhmer, J. Langridge, B. Connolly, T. Chadick, K. Holly, J. Eckels, E. W. Deutsch, R. L. Moritz, J. E. Katz, D. B. Agus, M. MacCoss, D. L. Tabb and P. Mallick (2012). "A cross-platform toolkit for mass spectrometry and proteomics." *Nat Biotechnol* **30**(10): 918-920.
- Chasseaud, L. F. (1979). "The role of glutathione and glutathione S-transferases in the metabolism of chemical carcinogens and other electrophilic agents." *Adv Cancer Res* **29**: 175-274.
- Consortium, I. H. G. (2019). "Comparative genomics of the major parasitic worms." *Nat Genet* **51**(1): 163-174.
- Dauguschies, A. and A. Joachim (2000). "Eicosanoids in parasites and parasitic infections." *Adv Parasitol* **46**: 181-240.
- DeLano, W. L. (2002). "The PyMOL Molecular Graphics System." from <http://www.pymol.org>.
- Diemert, D. J., M. E. Bottazzi, J. Plieskatt, P. J. Hotez and J. M. Bethony (2018). "Lessons along the Critical Path: Developing Vaccines against Human Helminths." *Trends in Parasitology* **34**(9): 747-758.
- Dunker, A. K., I. Silman, V. N. Uversky and J. L. Sussman (2008). "Function and structure of inherently disordered proteins." *Current Opinion in Structural Biology* **18**(6): 756-764.
- Faveeuw, C., T. Malleveay, K. Paschinger, I. Wilson, J. Fontaine, R. Mollicone, R. Oriol, F. Altmann, P. Lerouge, M. Capron and F. Trottein (2003). Schistosome N-glycans containing core α 3-fucose and core β 2-xylose epitopes are strong inducers of Th2 responses in mice.
- Feng, Z. P., X. Zhang, P. Han, N. Arora, R. F. Anders and R. S. Norton (2006). "Abundance of intrinsically unstructured proteins in *P. falciparum* and other apicomplexan parasite proteomes." *Mol Biochem Parasitol* **150**(2): 256-267.
- Graham, S. P., Y. Wu, K. Henkle-Duehrsen, S. Lustigman, T. R. Unnasch, G. Braun, S. A. Williams, J. McCarthy, A. J. Trees and A. E. Bianco (1999). "Patterns of *Onchocerca volvulus* recombinant antigen recognition in a bovine model of onchocerciasis." *Parasitology* **119 (Pt 6)**: 603-612.
- Guo, Y., H. Feinberg, E. Conroy, D. A. Mitchell, R. Alvarez, O. Blixt, M. E. Taylor, W. I. Weis and K. Drickamer (2004). "Structural basis for distinct ligand-binding and targeting properties of the receptors DC-SIGN and DC-SIGNR." *Nat Struct Mol Biol* **11**(7): 591-598.

Habig, W. H., M. J. Pabst and W. B. Jakoby (1974). "Glutathione S-transferases. The first enzymatic step in mercapturic acid formation." *J Biol Chem* **249**(22): 7130-7139.

Hayes, J. D., J. U. Flanagan and I. R. Jowsey (2005). "Glutathione transferases." *Annu Rev Pharmacol Toxicol* **45**: 51-88.

Howe, K. L., B. J. Bolt, M. Shafie, P. Kersey and M. Berriman (2017). "WormBase ParaSite - a comprehensive resource for helminth genomics." *Mol Biochem Parasitol* **215**: 2-10.

Inoue, T., D. Irikura, N. Okazaki, S. Kinugasa, H. Matsumura, N. Uodome, M. Yamamoto, T. Kumasaka, M. Miyano, Y. Kai and Y. Urade (2003). "Mechanism of metal activation of human hematopoietic prostaglandin D synthase." *Nat Struct Biol* **10**(4): 291-296.

Jakoby, W. B. and W. H. Habig (1980). Chapter 4 - Glutathione Transferases. *Enzymatic Basis of Detoxication*. W. B. Jakoby, Academic Press: 63-94.

Jaurigue, J. A. and P. H. Seeberger (2017). "Parasite Carbohydrate Vaccines." *Frontiers in cellular and infection microbiology* **7**: 248-248.

Joachim, A. and B. Ruttkowski (2011). "Prostaglandin D(2) synthesis in *Oesophagostomum dentatum* is mediated by cytosolic glutathione S-transferase." *Exp Parasitol* **127**(2): 604-606.

Kallberg, M., H. Wang, S. Wang, J. Peng, Z. Wang, H. Lu and J. Xu (2012). "Template-based protein structure modeling using the RaptorX web server." *Nat Protoc* **7**(8): 1511-1522.

Kelley, L. A., S. Mezulis, C. M. Yates, M. N. Wass and M. J. E. Sternberg (2015). "The Phyre2 web portal for protein modeling, prediction and analysis." *Nature Protocols* **10**: 845.

Kozak, R. P., C. B. Tortosa, D. L. Fernandes and D. I. Spencer (2015). "Comparison of procainamide and 2-aminobenzamide labeling for profiling and identification of glycans by liquid chromatography with fluorescence detection coupled to electrospray ionization-mass spectrometry." *Anal Biochem* **486**: 38-40.

Kubata, B. K., M. Duzenko, K. S. Martin and Y. Urade (2007). "Molecular basis for prostaglandin production in hosts and parasites." *Trends Parasitol* **23**(7): 325-331.

Kutyrev, I. A., N. M. Biserova, D. N. Olennikov, J. V. Korneva and O. E. Mazur (2017). "Prostaglandins E2 and D2-regulators of host immunity in the model parasite *Diphylobothrium dendriticum*: An immunocytochemical and biochemical study." *Mol Biochem Parasitol* **212**: 33-45.

Laan, L. C., A. R. Williams, K. Stavenhagen, M. Giera, G. Kooij, I. Vlasakov, H. Kalay, H. Kringel, P. Nejsun, S. M. Thamsborg, M. Wuhrer, C. D. Dijkstra, R. D. Cummings and I. van Die (2017). "The whipworm (*Trichuris suis*) secretes prostaglandin E2 to suppress proinflammatory properties in human dendritic cells." *Faseb j* **31**(2): 719-731.

LaCourse, E. J., M. Hernandez-Viadel, J. R. Jefferies, C. Svendsen, D. J. Spurgeon, J. Barrett, A. J. Morgan, P. Kille and P. M. Brophy (2009). "Glutathione transferase (GST) as a candidate molecular-based biomarker for soil toxin exposure in the earthworm *Lumbricus rubellus*." *Environ Pollut* **157**(8-9): 2459-2469.

LaCourse, E. J., S. Perally, R. M. Morphew, J. V. Moxon, M. Prescott, D. J. Dowling, S. M. O'Neill, A. Kipar, U. Hetzel, E. Hoey, R. Zafra, L. Buffoni, J. Perez Arevalo and P. M. Brophy (2012). "The Sigma class glutathione transferase from the liver fluke *Fasciola hepatica*." *PLoS Negl Trop Dis* **6**(5): e1666.

Laemmli, U. K. (1970). "Cleavage of structural proteins during the assembly of the head of bacteriophage T4." *Nature* **227**(5259): 680-685.

Larkin, M. A., G. Blackshields, N. P. Brown, R. Chenna, P. A. McGettigan, H. McWilliam, F. Valentin, I. M. Wallace, A. Wilm, R. Lopez, J. D. Thompson, T. J. Gibson and D. G. Higgins (2007). "Clustal W and Clustal X version 2.0." *Bioinformatics* **23**(21): 2947-2948.

Liebau, E., G. Wildenburg, R. D. Walter and K. Henkle-Duhrsen (1994). "A novel type of glutathione S-transferase in *Onchocerca volvulus*." *Infect Immun* **62**(11): 4762-4767.

Line, K., M. N. Isupov, E. J. LaCourse, D. J. Cutress, R. M. Morphew, P. M. Brophy and J. A. Littlechild (2019). "X-ray structure of *Fasciola hepatica* Sigma class glutathione transferase 1 reveals a disulfide bond to support stability in gastro-intestinal environment." *Scientific Reports* **9**(1): 902.

Lopes, J. L. S., D. Orcia, A. P. U. Araujo, R. DeMarco and B. A. Wallace (2013). "Folding factors and partners for the intrinsically disordered protein micro-exon gene 14 (MEG-14)." *Biophysical journal* **104**(11): 2512-2520.

Luk, F. C., T. M. Johnson and C. J. Beckers (2008). "N-linked glycosylation of proteins in the protozoan parasite *Toxoplasma gondii*." *Mol Biochem Parasitol* **157**(2): 169-178.

Makepeace, B. L. and V. N. Tanya (2016). "25 Years of the *Onchocerca ochengi* Model." Trends in Parasitology **32**(12): 966-978.

Meyer, D. J., R. Muimo, M. Thomas, D. Coates and R. E. Isaac (1996). "Purification and characterization of prostaglandin-H E-isomerase, a sigma-class glutathione S-transferase, from *Ascaridia galli*." Biochem J **313** (Pt 1): 223-227.

Meyer, D. J. and M. Thomas (1995). "Characterization of rat spleen prostaglandin H D-isomerase as a sigma-class GSH transferase." Biochem J **311** (Pt 3): 739-742.

Perbandt, M., J. Hoppner, C. Burmeister, K. Luersen, C. Betzel and E. Liebau (2008). "Structure of the extracellular glutathione S-transferase OvGST1 from the human pathogenic parasite *Onchocerca volvulus*." J Mol Biol **377**(2): 501-511.

Ruy, P. d. C., R. Torrieri, J. S. Toledo, V. d. S. Alves, A. K. Cruz and J. C. Ruiz (2014). "Intrinsically disordered proteins (IDPs) in trypanosomatids." BMC Genomics **15**(1): 1100.

Sankari, T., S. L. Hoti, L. K. Das, V. Govindaraj and P. K. Das (2013). "Effect of Diethylcarbamazine (DEC) on prostaglandin levels in *Wuchereria bancrofti* infected microfilaraemics." Parasitol Res **112**(6): 2353-2359.

Schmidt, R., O. Coste and G. Geisslinger (2005). "LC-MS/MS-analysis of prostaglandin E2 and D2 in microdialysis samples of rats." J Chromatogr B Analyt Technol Biomed Life Sci **826**(1-2): 188-197.

Sheehan, D., G. Meade, V. M. Foley and C. A. Dowd (2001). "Structure, function and evolution of glutathione transferases: implications for classification of non-mammalian members of an ancient enzyme superfamily." Biochem J **360**(Pt 1): 1-16.

Simons, P. C. and D. L. Vander Jagt (1977). "Purification of glutathione S-transferases from human liver by glutathione-affinity chromatography." Anal Biochem **82**(2): 334-341.

Sommer, A., M. Nimtz, H. S. Conradt, N. Brattig, K. Boettcher, P. Fischer, R. D. Walter and E. Liebau (2001). "Structural analysis and antibody response to the extracellular glutathione S-transferases from *Onchocerca volvulus*." Infect Immun **69**(12): 7718-7728.

Sommer, A., R. Rickert, P. Fischer, H. Steinhart, R. D. Walter and E. Liebau (2003). "A Dominant Role for Extracellular Glutathione Transferase from *Onchocerca volvulus* Is the Production of Prostaglandin D." Infection and Immunity **71**(6): 3603-3606.

Szkudlinski, J. (2000). "Occurrence of prostaglandins and other eicosanoids in parasites and their role in host-parasite interaction." Wiad Parazytol **46**(4): 439-446.

Taylor, P. R., L. Martinez-Pomares, M. Stacey, H. H. Lin, G. D. Brown and S. Gordon (2005). "Macrophage receptors and immune recognition." Annu Rev Immunol **23**: 901-944.

Thompson, J. D., T. J. Gibson, F. Plewniak, F. Jeanmougin and D. G. Higgins (1997). "The CLUSTAL_X windows interface: flexible strategies for multiple sequence alignment aided by quality analysis tools." Nucleic Acids Res **25**(24): 4876-4882.

Trees, A. J. (1992). "*Onchocerca ochengi*: Mimic, model or modulator of *O. volvulus*?" Parasitology Today **8**(10): 337-339.

Trees, A. J., S. P. Graham, A. Renz, A. E. Bianco and V. Tanya (2000). "*Onchocerca ochengi* infections in cattle as a model for human onchocerciasis: recent developments." Parasitology **120** Suppl: S133-142.

Uversky, V. N. (2013). "The alphabet of intrinsic disorder: II. Various roles of glutamic acid in ordered and intrinsically disordered proteins." Intrinsically disordered proteins **1**(1): e24684-e24684.

van der Lee, R., M. Buljan, B. Lang, R. J. Weatheritt, G. W. Daughdrill, A. K. Dunker, M. Fuxreiter, J. Gough, J. Gsponer, D. T. Jones, P. M. Kim, R. W. Kriwacki, C. J. Oldfield, R. V. Pappu, P. Tompa, V. N. Uversky, P. E. Wright and M. M. Babu (2014). "Classification of intrinsically disordered regions and proteins." Chemical reviews **114**(13): 6589-6631.

Vizcaino, J. A., A. Csordas, N. del-Toro, J. A. Dianas, J. Griss, I. Lavidas, G. Mayer, Y. Perez-Riverol, F. Reisinger, T. Ternent, Q. W. Xu, R. Wang and H. Hermjakob (2016). "2016 update of the PRIDE database and its related tools." Nucleic Acids Res **44**(D1): D447-456.

WHO. (2018). "Onchocerciasis Fact Sheet." from <https://www.who.int/news-room/fact-sheets/detail/onchocerciasis>.

Wright, P. E. and H. J. Dyson (2015). "Intrinsically disordered proteins in cellular signalling and regulation." Nature reviews. Molecular cell biology **16**(1): 18-29.

Xu, D. and Y. Zhang (2011). "Improving the physical realism and structural accuracy of protein models by a two-step atomic-level energy minimization." *Biophys J* **101**(10): 2525-2534.

Yang, J., R. Yan, A. Roy, D. Xu, J. Poisson and Y. Zhang (2015). "The I-TASSER Suite: protein structure and function prediction." *Nat Methods* **12**(1): 7-8.

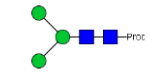
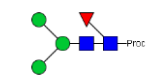
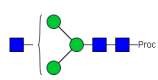
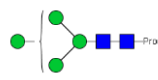
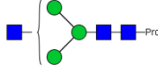
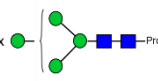
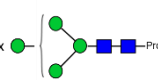

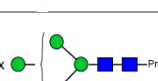
Accepted Manuscript

Table 1. List of the most abundant proteins detected by mass spectrometry from in-gel analyses of *O. ochengi* GST

Spot Number	WormBase ID	Description	GST class	Score	% coverage	Predicted Mr (kDa)	Predicted PI	Peptide Sequence
1	1::nOo.2.0.1.t00341	glutathione transferase	Pi	70	24	24.4	7.3	R.LFLVDQDIK.F R.MIYMAYETEKDPYIK.S K.SQFQFGQLPCLYDGDQQIVQSGAILR.H
2	1::nOo.2.0.1.t00341	glutathione transferase	Pi	49	19	24.4	7.3	K.LTYFSIR.G K.SILPGELAK.F R.LFLVDQDIK.F R.MIYMAYETEKDPYIK.S
3	1::nOo.2.0.1.t00341	glutathione transferase	Pi	70	42	24.4	7.3	K.LTYFSIR.G K.SILPGELAK.F R.LFLVDQDIK.F R.MIYMAYETEKDPYIK.S R.KYNLNGENEMETTYIDMFCEGVR.D K.SQFQFGQLPCLYDGDQQIVQSGAILR.H
4	1::nOo.2.0.1.t00341	glutathione transferase	Pi	91	42	24.4	7.3	K.LTYFSIR.G K.SILPGELAK.F R.LFLVDQDIK.F R.MIYMAYETEK.S R.MIYMAYETEKDPYIK.S R.KYNLNGENEMETTYIDMFCEGVR.D K.SQFQFGQLPCLYDGDQQIVQSGAILR.H
5	1::nOo.2.0.1.t00341	glutathione transferase	Pi	150	42	24.4	7.3	K.LTYFSIR.G K.SILPGELAK.F R.LFLVDQDIK.F R.MIYMAYETEK.S R.MIYMAYETEKDPYIK.S K.YNLNGENEMETTYIDMFCEGVR.D R.KYNLNGENEMETTYIDMFCEGVR.D K.SQFQFGQLPCLYDGDQQIVQSGAILR.H

6	1::nOo.2.0.1.t00341	glutathione transferase	Pi	259	42	24.4	7.3	K.LTYFSIR.G K.SILPGELAK.F R.LFLVDQDIK.F R.MIYMAYETEK.S R.MIYMAYETEKDPYIK.S K.YNLNGENEMETTYIDMFCEGVR.D K.SQFQFGQLPCLYDGDQIQVQSGAILR.H
7	1::nOo.2.0.1.t00341	glutathione transferase	Pi	30	24	24.4	7.3	R.LFLVDQDIK.F R.MIYMAYETEKDPYIK.S K.SQFQFGQLPCLYDGDQIQVQSGAILR.H
8	1::nOo.2.0.1.t00341	glutathione transferase	Pi	43		24.4	7.3	K.SILPGELAK.F R.LFLVDQDIK.F R.MIYMAYETEKDPYIK.S
9	1::nOo.2.0.1.t00341	glutathione transferase	Pi	49	4	24.4	7.3	K.SILPGELAK.F R.LFLVDQDIK.F
10	1::nOo.2.0.1.t09064	glutathione s-transferase 1	Sigma	231	34	28.5	9.4	K.IGQMPGIK.E K.LIPWTHEK.N K.YTLTYFNNGR.N R.FGLLGTNAWEEAK.I K.LEEYPQLASFVNK.I K.IMAVVLNIEELFQK.L K.VSVADLAVFNMLMTLDDQVK.L
11	1::nOo.2.0.1.t00341	glutathione transferase	Pi	109	19	24.4	7.3	K.LTYFSIR.G K.SILPGELAK.F R.LFLVDQDIK.F R.MIYMAYETEKDPYIK.S

Table 2. Summary of most abundant N-glycan species from OoGST1. Proposed structures and relative abundance of the most common glycans from OoGST1 were taken from HILIC-LC (Fig. 6), and EIS-MS (Fig. S1) and EIS-MS/MS (Fig. 7) analyses.

Peak No.	GU	% Relative Abundance	Detected [M+Proc+2H ⁺] ²⁺	Detected [M+Proc+H ⁺] ¹⁺	Theoretical [M+Proc+H ⁺] ¹⁺	Composition	Proposed Structure
14	4.21	7.7	565.84	1130.67	1130.5	(Hex) ₃ (HexNAc) ₂	
17	4.64	0.7	637.67	1276.69	1276.6	(Hex) ₃ (HexNAc) ₂ (Deoxyhexose) ₁	
18	4.79	3.2	ND	1333.71	1333.3	(Hex) ₃ (HexNAc) ₃	
20	5.03	19.7	646.87	1292.73	1292.3	(Hex) ₄ (HexNAc) ₂	
21	5.34	1.8	767.90	ND	1536.3	(Hex) ₃ (HexNAc) ₄	2x 
26	5.99	45.2	727.89	1454.78	1454.3	(Hex) ₅ (HexNAc) ₂	5x 
33	6.89	12.0	808.92	ND	1616.3	(Hex) ₆ (HexNAc) ₂	6x 
39	7.81	6.1	889.83	ND	1778.3	(Hex) ₇ (HexNAc) ₂	7x 
44	8.67	0.5	971.02	ND	1940.3	(Hex) ₈ (HexNAc) ₂	8x 

46	9.39	3.1	1054.55	ND	2102.3	(Hex) ₉ (HexNAc) ₂	
----	------	-----	---------	----	--------	--	--

■ GlcNAc
 ○ Mannose
 ▽ Fucose

Accepted Manuscript

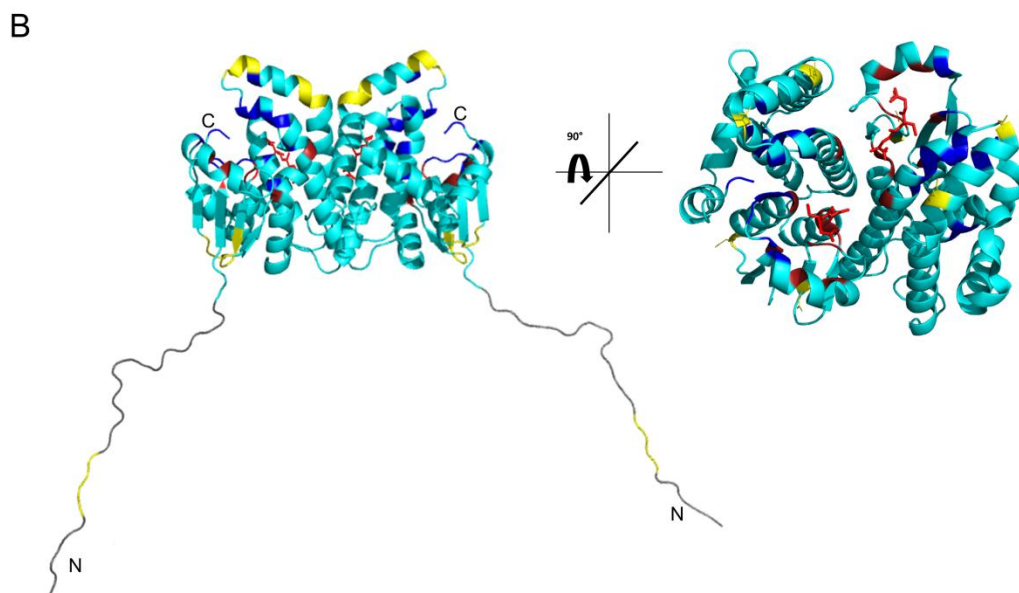
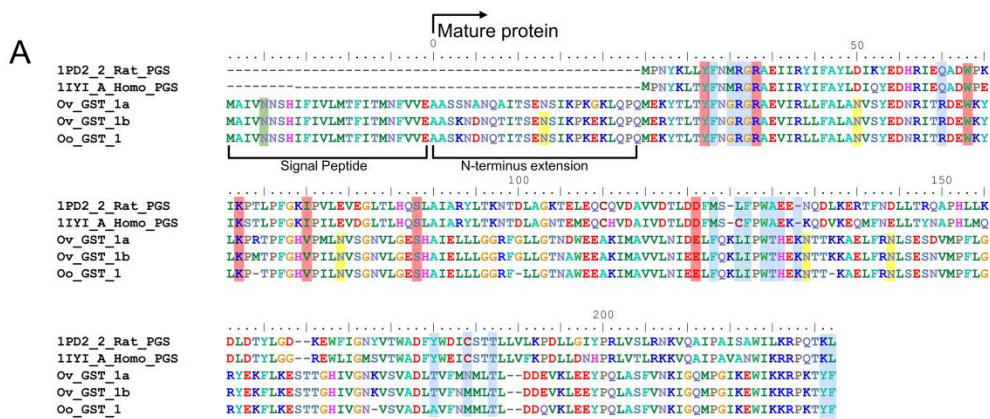


Fig. 1. *in silico* analyses of *O. ochengi* sigma class GST OoGST1. **A**, alignment of amino acid sequences of OoGST1 with homologues from its sister species *O. volvulus*, and PGDS from rat and human. Blue boxes show the regions that are predicted to form the PDH₂ binding pocket across rat, human and *O. volvulus* sigma class GST (information adapted from (Perbandt, Hoppner et al. 2008)). Yellow boxes highlight the predicted *N*-glycosylation sites in the mature *Onchocerca* spp. GSTs, whilst green box highlights a predicted *N*-glycosylation site in the cleavable signal peptide. Red boxes indicate the GSH binding regions. Global alignment was produced using ClustalX Version 2.1 (Thompson *et al.*, 1997; Larkin *et al.*, 2007). Accession numbers for the proteins used in the alignment are as follows; 1PD2_2_Rat_PGS – gi:6435744 (1PD2_2) from *Rattus norvegicus*; 1IYI_A_Homo_PGS – gi:30749302 (1IYI_A) from *Homo sapiens*; Ov_GST_1a – gi:12005978 (AAG44695.1) from *Onchocerca volvulus*; Ov_GST_1b – gi:12005978 (AAG44695.1) from *Onchocerca volvulus*; nOo.2.0.1.t09064–WormBase ParaSite (Armstrong et al 2016). **B**, This initial model produced *in silico* using SwissModel (Arnold *et al* 2006) is based upon alignment of the *O. ochengi* sequence with the Protein Databank template pdb.2HNL from the closely related *Onchocerca volvulus* sigma GST. The dimeric protein model is shown here with the 25 disordered amino acids N-terminal extension. Blue, yellow and red are used to highlight the PDH₂ binding pocket, predicted *N*-glycosylation sites and GSH binding sites respectively. Rotating the protein 90° shows the wide PDH₂ binding pockets, revealing bound GSH (red ball and stick).

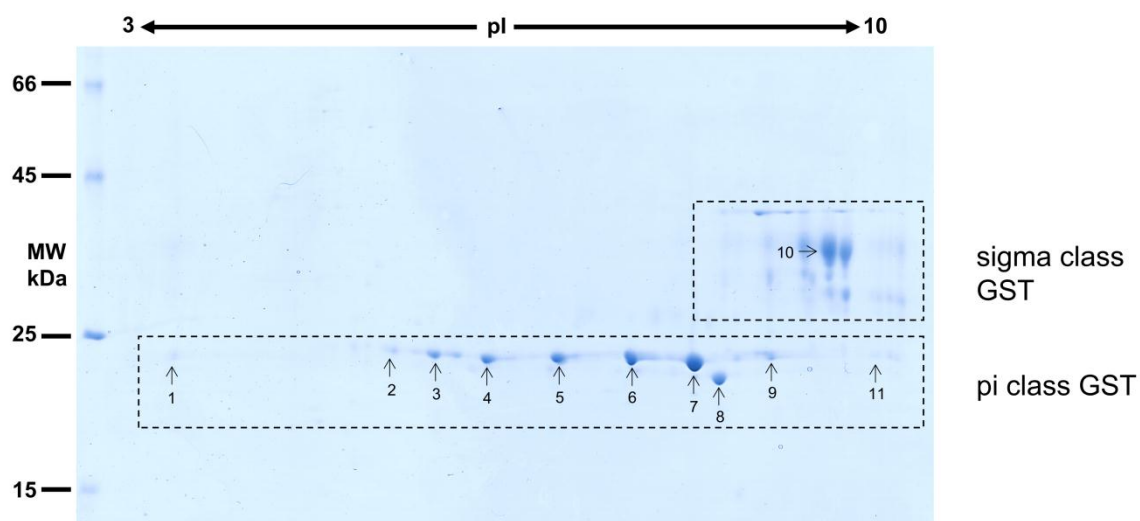


Fig. 2. 2DE analysis of cytosolic glutathione-binding proteins of *O. ochengi*. 20 μ g of S-HexylGSH purified GSTs were resolved via 2DE. Numbers/arrows indicate spots excised from the 2DE gel and identified via mass spectrometry (Table 1 and supplementary file 1). Gel represents one of three run independently with the same sample, with identified spots visualised in all three gels.

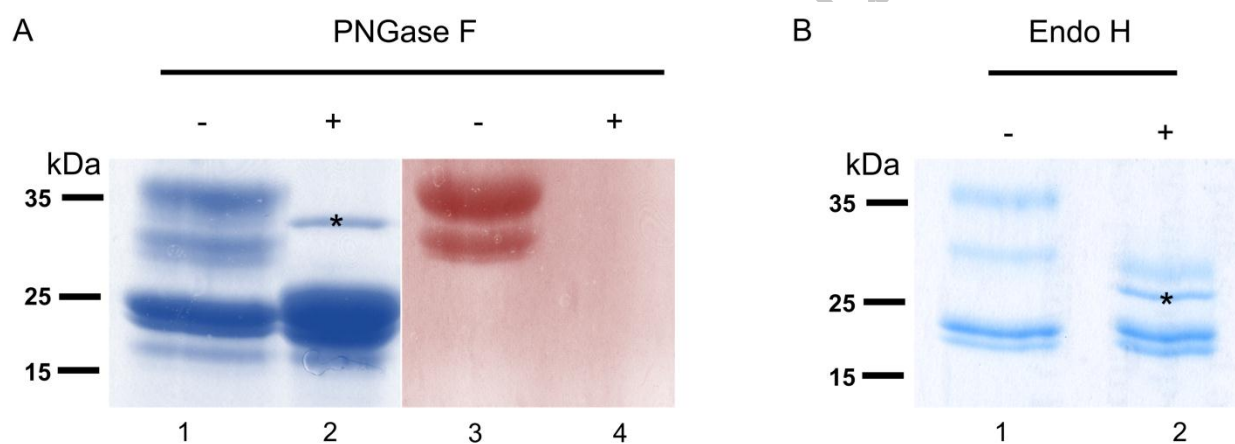


Fig. 3. Glycosylated status of S-hexylGSH-purified *O. ochengi* GSTs. (A), 5 μ g of undigested (lanes 1 and 3) or PNGase F-treated (lanes 2 and 4) GSTs were fractionated on 12.5% SDS-PAGE and stained with either colloidal Coomassie blue (lanes 1 and 2) or PAS (lanes 3 and 4). The asterisk (*) in lane 2 shows migration of PNGase F enzyme. (B), Lanes 1 and 2 show non-glycosidase-digested and Endo H-treated GSTs from *O. ochengi* respectively. The asterisk (*) in lane 2 shows Coomassie staining of the glycosidase Endo H enzyme.

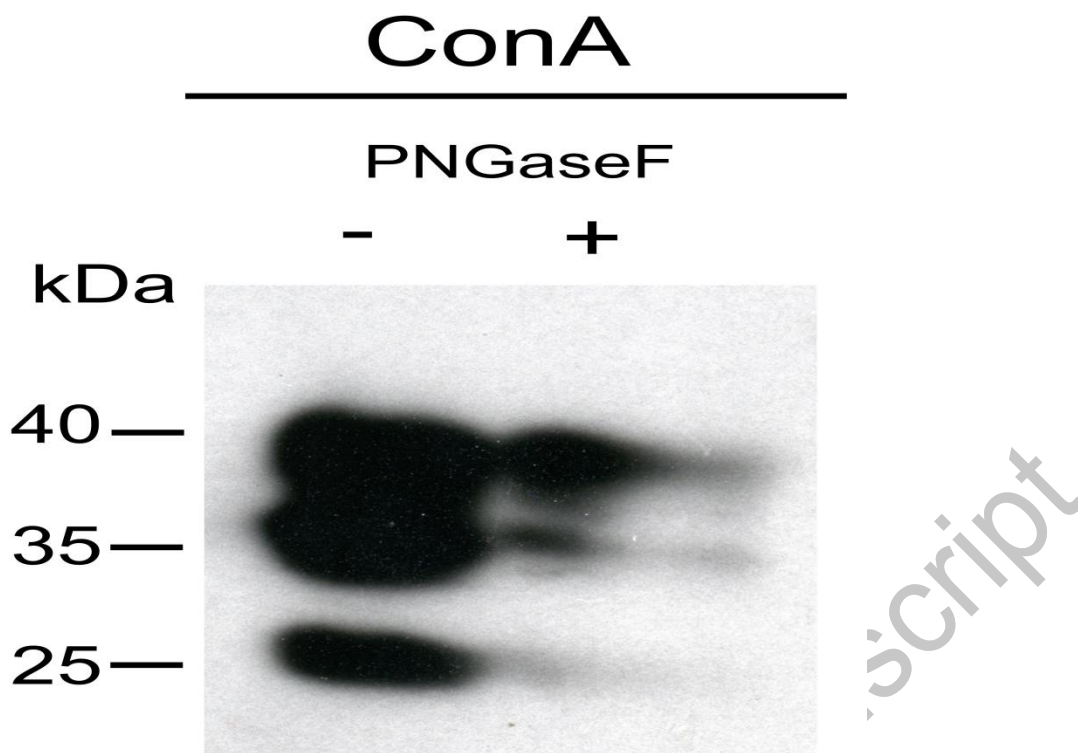


Fig. 4. Lectin-affinity blotting of *O. ochengi* GST. Undigested (-) or PNGaseF-treated (+) GSTs were fractionated by SDS-PAGE, transferred to a nitrocellulose membrane and incubated with ConA for detection of mannose.

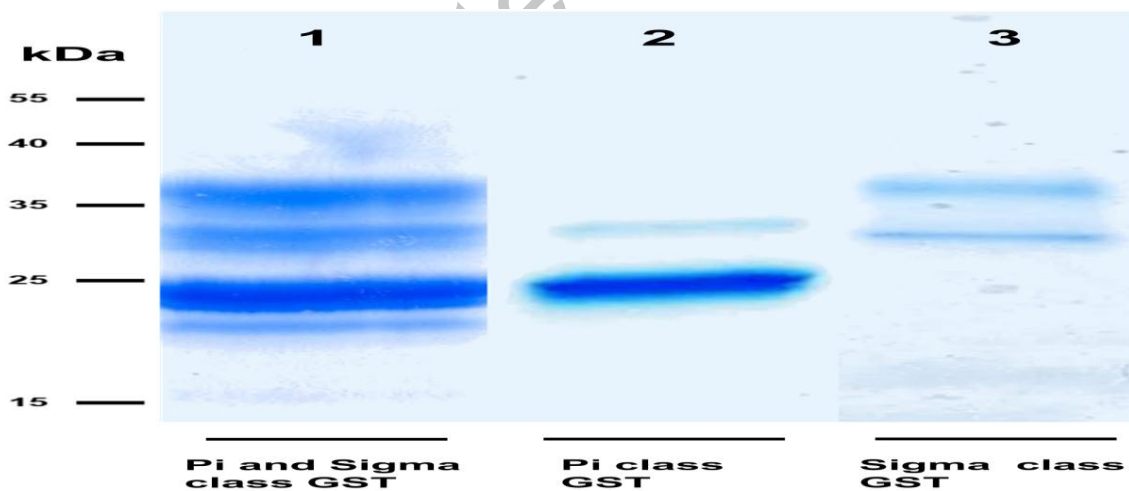


Fig. 5. SDS PAGE gel showing *O. ochengi* glutathione transferases (GSTs), resolved via S-hexylGSH-affinity and ConA-lectin-affinity chromatography. All bands shown in the SDS PAGE image were glutathione transferases (GSTs) of pi and sigma classes, purified and identified via tandem mass spectrometry. Lane 1, GSTs of pi and sigma classes resolved from cytosolic extracts eluted from a S-hexylGSH-affinity column. Lane 2, S-hexylGSH-affinity GSTs of the pi class that do not bind to the ConA-lectin-affinity column. Lane 3, ConA-lectin-binding sigma class GSTs that also bind the S-hexylGSH-affinity column.

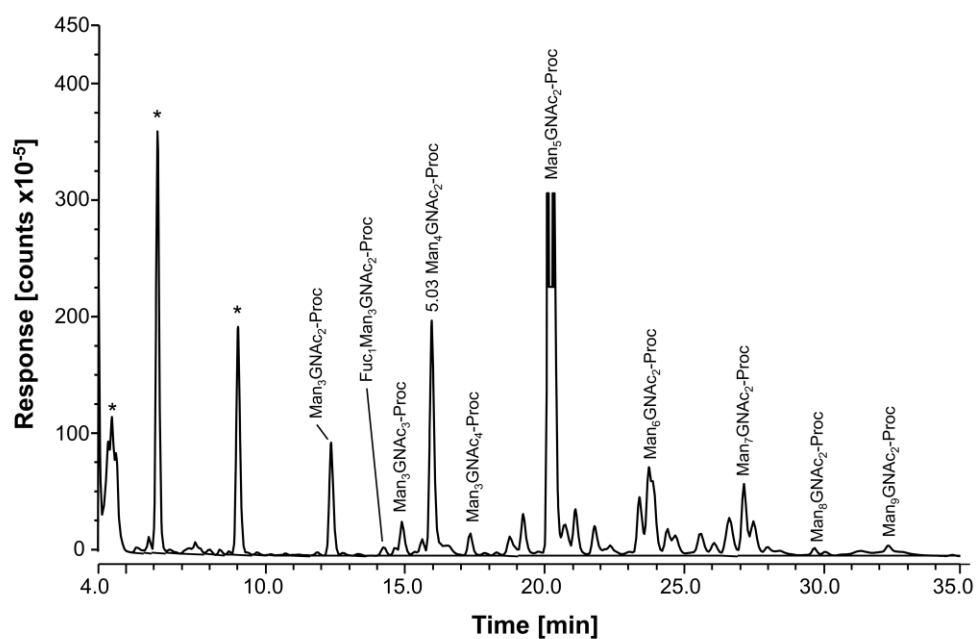


Fig. 6. HILIC-LC separation of procainamide labelled *N*-glycans from *O. ochengi* GST1. Asterisks indicate contaminants (mainly from chitin hydrolysate ladder).

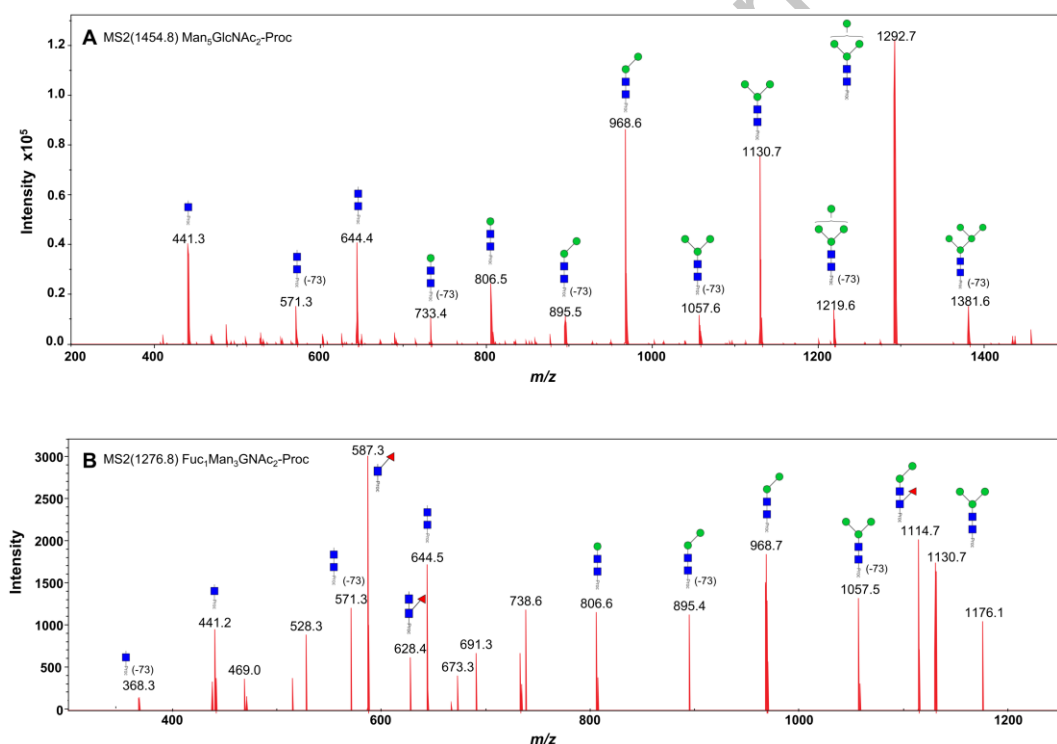


Fig. 7. Positive-ion MS/MS spectra of $\text{Man}_5\text{GlcNAc}_2\text{-Proc}$ (A) and $\text{Fuc}_1\text{Man}_3\text{GlcNAc}_2\text{-Proc}$ (B) from *O. ochengi* GST1. (-73) refers to $[\text{M}+\text{H}]^+$ ions that have lost terminal diethylamine from the procainamide tag during collision (Kozak, Tortosa et al. 2015). Blue squares, *N*-acetylglucosamine residues; green circles, mannose residues; red triangles, fucose residues; Proc, procainamide tag.

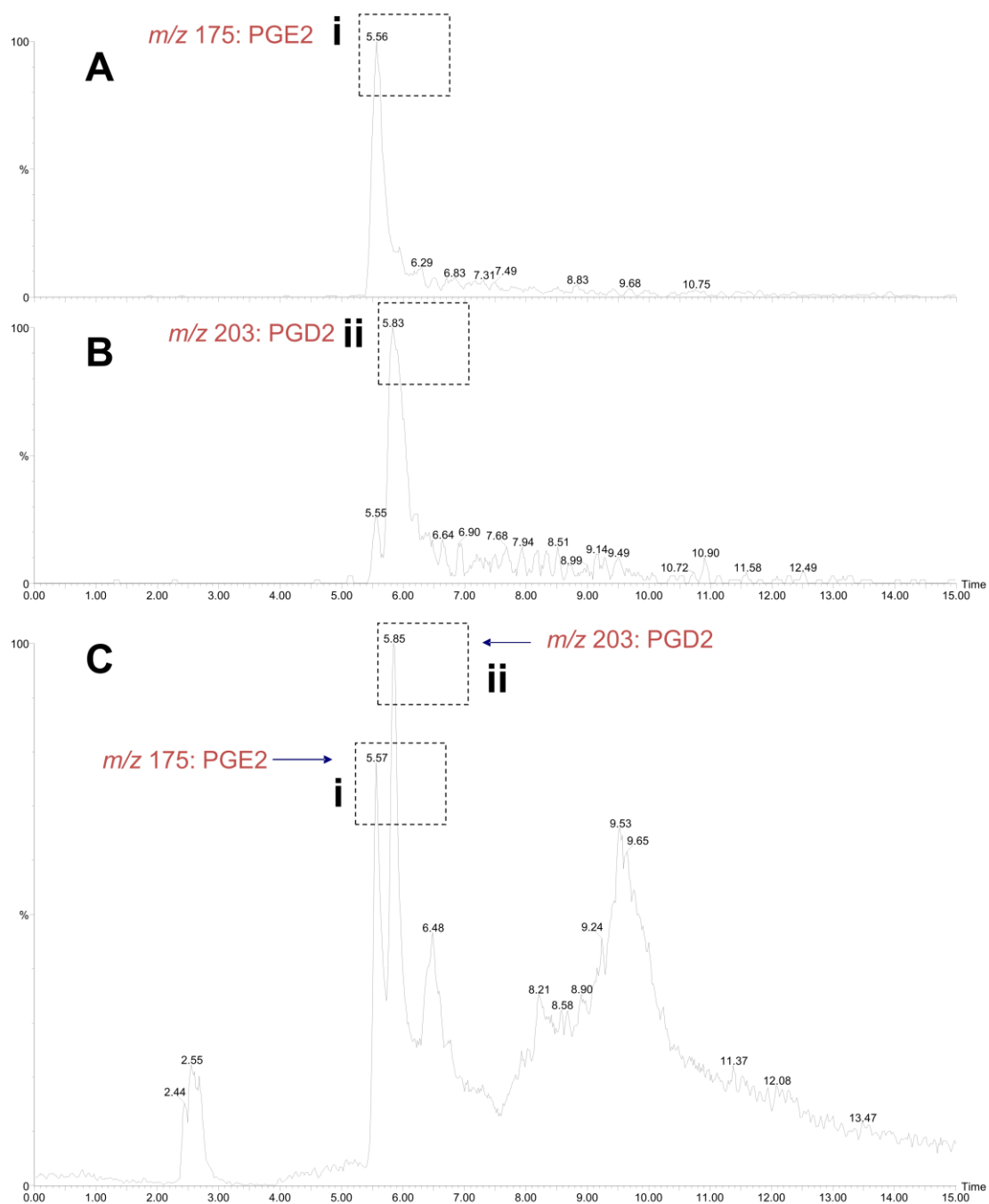


Fig. 8. Detection of prostaglandin synthase activity of *O. ochengi* sigma class GST via a mass spectrometry approach. A coupled assay with *O. ochengi* native sigma class GST and COX-1 catalyses the conversion of arachidonic acid to the H2 form before the prostaglandin isomer is converted to either the D or E form. Nano-LC/MS analysis allowed detection of both PGE2 (A) and PGD2 (B) in the assay mixture with the PGD2 form being the more abundant of the two prostanoids (C). Dashed, boxed figures above peaks show the fragmentation ions specific to detection of PGE2 (i) and PGD2 (ii) according to the method used and described by LaCourse *et al* (LaCourse, Perally *et al.* 2012).